Crystal chemistry of anhydrous Li uranyl phosphates and arsenates. I. Polymorphism and structure topology: Synthesis and crystal structures of α-Li[(UO$_2$)(PO$_4$)], α-Li[(UO$_2$)(AsO$_4$)], β-Li[(UO$_2$)(AsO$_4$)] and Li$_2$[(UO$_2$)$_3$(P$_2$O$_7$)$_2$]

Evgeny V. Alekseev [a,b,*], Sergey V. Krivovichev [c], Thomas Malcherek [d], Wulf Depmeier [a]

[a] Institut für Geowissenschaften, Universität Kiel, D-24118 Kiel, Germany
[b] Nizhny Novgorod State University, 603950 Nizhny Novgorod, Russia
[c] Department of Crystallography, St. Petersburg State University, 199034 St. Petersburg, Russia
[d] Mineralogisch-Petrographisches Institut, Universität Hamburg, Grindelallee 48, D-20146 Hamburg, Germany

ARTICLE INFO

ABSTRACT

Four new Li uranyl phosphates and arsenates have been prepared by high-temperature solid-state reactions: α-Li[(UO$_2$)(PO$_4$)] (1), α-Li[(UO$_2$)(AsO$_4$)] (2), β-Li[(UO$_2$)(AsO$_4$)] (3) and Li$_2$[(UO$_2$)$_3$(P$_2$O$_7$)$_2$] (4). The structures of the compounds have been solved by direct methods: 1—triclinic, $P\bar{1}$, $a = 5.0271(1)$ Å, $b = 9.8799(2)$ Å, $c = 10.8920(2)$ Å, $\alpha = 108.282(9)°$, $\beta = 102.993(8)°$, $\gamma = 104.13(1)°$, $V = 470.69(3)$ Å^3, $Z = 4$, $R_1 = 0.0415$ for 2786 unique reflections with $|F_0| \geqslant 4\sigma_F$; 2—triclinic, $P\bar{1}$, $a = 5.129(2)$ Å, $b = 10.105(3)$ Å, $c = 11.080(3)$ Å, $\alpha = 107.70(2)°$, $\beta = 102.53(3)°$, $\gamma = 104.74(3)°$, $V = 501.4(3)$ Å^3, $Z = 4$, $R_1 = 0.055$ for 1431 unique reflections with $|F_0| \geqslant 4\sigma_F$; 3—triclinic, $P\bar{1}$, $a = 5.051(1)$ Å, $b = 5.303(1)$ Å, $c = 10.101(1)$ Å, $\alpha = 90.31(1)°$, $\beta = 97.49(1)°$, $\gamma = 105.08(1)°$, $V = 258.80(8)$ Å^3, $Z = 2$, $R_1 = 0.0339$ for 2055 unique reflections with $|F_0| \geqslant 4\sigma_F$; 4—triclinic, $P\bar{1}$, $a = 5.312(1)$ Å, $b = 6.696(1)$ Å, $c = 12.542(1)$ Å, $\alpha = 94.532(9)°$, $\beta = 99.059(8)°$, $\gamma = 110.189(7)°$, $V = 409.17(10)$ Å^3, $Z = 2$, $R_1 = 0.0565$ for 1355 unique reflections with $|F_0| \geqslant 4\sigma_F$. The structures of all four compounds are based upon 3-D frameworks of U and T polyhedra ($T = $ P, As). Phases 1 and 2 are isostructural and consist of U$_2$O$_{12}$ dimers and UO$_6$ square bipyramids linked by single TO$_4$ tetrahedra. The structure of 3 consists of 3-D framework of corner-sharing UO$_6$ bipyramids and AsO$_4$ tetrahedra. In the structure of 4, the framework is composed of U$_2$O$_{12}$ dimers, UO$_6$ bipyramids and P$_2$O$_7$ dimers. In all the compounds, Li$^+$ cations reside in framework cavities. The topologies of the 3-D frameworks can be described as derivatives of the PtS (cooperite) network.

1. Introduction

The structural chemistry of uranium compounds is developing quickly, owing to the challenges related with nuclear energy, material and environmental applications [1–4]. Uranyl phosphates and arsenates are the most common uranium minerals. In nature, these phases usually contain water and most of them belong to the autunite and phosphuranylite mineral groups [5]. Although anhydrous uranyl phosphates and arsenates have also received certain attention [6–11], systematic structural studies of these phases are only beginning [12]. Recently, we have investigated a series of K uranyl arsenates and phosphates,

including the layered structure of K[(UO$_2$)(As$_2$O$_7$)] [13] with melilite-related topology, and framework structures of α,β-K[(UO$_2$)(P$_3$O$_9$)] and K[(UO$_2$)$_2$(P$_3$O$_{10}$)] [14]. Applications of symbolic descriptions of the uranyl phosphate and arsenate networks using graph theory provided unique insight into their structural architectures and allowed comparison of their structures with related compounds.

In continuation of our studies, we present here results on four new phases with the compositions α-Li[(UO$_2$)(PO$_4$)] (1), α-Li[(UO$_2$)(AsO$_4$)] (2), β-Li[(UO$_2$)(AsO$_4$)] (3) and Li$_2$[(UO$_2$)$_3$(P$_2$O$_7$)$_2$] (4). Again, graphical description of the uranyl arsenate and phosphate structural units allows to analyze topological relations between the different phases and to trace genealogies of the structural topologies. Here we shall demonstrate that the networks of U–T linkages ($T = $ P, As) in these compounds under consideration can be treated as modifications of the PtS (cooperite) net.

* Corresponding author at: Institut für Geowissenschaften, Universität Kiel, D-24118 Kiel, Germany. Fax: +49 431 880 4457.
E-mail address: e_v_alekseev@mail.ru (E.V. Alekseev).

2. Experimental

2.1. Synthesis

Crystals of the title compounds were obtained by high-temperature solid-state reactions. Mixtures of Li_2CO_3, $UO_2(NO_3)_2$, P_2O_5 or As_2O_5 taken in molar ratios of 1:1:2 for **1**, **2**, and **3** and 2:3:6 for **4**, were heated in a platinum crucible to 820 °C and then cooled to 50 °C with a cooling rate of 5 °C/h. The products consisted of greenish-yellow transparent crystals of **1**, **2**, **3** and **4**.

2.2. Crystal-structure analysis

The crystals selected for data collection were mounted on an Enraf-Nonius Kappa CCD (**1**), Stoe Stadi-4 (**2** and **3**) and on Mar345 Image Plate (**4**) diffractometers. All data were collected using monochromatic MoKα X-radiation. The unit-cell dimensions for all compounds (Table 1) were refined using least-squares techniques. More than a hemisphere of data was collected for each crystal and the three-dimensional data were reduced and filtered for statistical outliers using the supporting programs for diffract-ometers. Data were corrected for Lorentz, polarization, absorption and background effects. Additional information pertinent to the data collection is given in Table 1.

The SHELXL 97 program was used for the determination and refinement of the structures. The structures were solved by direct methods and refined to $R_1 = 0.045$ for **1**, 0.055 for **2**, 0.0339 for **3** and 0.0565 for **4**. The final models included anisotropic displacement parameters for all atoms (except Li) and weighting schemes of the structure factors. The final atomic positional and displacement parameters, and selected interatomic distances are given in Tables 2 and 6 for **1**, 3 and 7 for **2**, 4 and 8 for **3**, 5 and 9 for **4**. Tables of observed and calculated structure factors for each structure are available from the authors upon request.

3. Results

3.1. Cation coordination

The uranium atoms in **1**, **2** and **4** have two types of coordination geometries: square bipyramidal and pentagonal

Table 2
Atomic coordinates and displacement parameters (Å^2) for **1**

Atom	x	y	z	U_{eq}
U(1)	0.03259(9)	0.79585(5)	0.02086(4)	0.00628(9)
U(2)	−0.02230(9)	0.72020(5)	0.48380(4)	0.00678(9)
P(1)	0.2758(6)	0.5840(3)	0.2205(3)	0.0060(5)
P(2)	0.3397(7)	1.1093(3)	0.2655(3)	0.0063(5)
Li(1)	0.736(6)	0.905(3)	0.303(3)	0.022(6)
Li(2)	0.677(6)	0.380(3)	0.228(3)	0.022(6)
O(1)	−0.210(2)	0.811(1)	0.1184(9)	0.011(2)
O(2)	0.622(2)	1.248(1)	0.338(1)	0.011(2)
O(3)	0.130(2)	1.119(1)	0.350(1)	0.014(2)
O(4)	0.045(2)	0.563(1)	0.2933(9)	0.012(2)
O(5)	0.566(2)	0.703(1)	0.3258(9)	0.012(2)
O(6)	0.269(2)	0.778(1)	−0.076(1)	0.018(2)
O(7)	0.185(2)	1.096(1)	0.121(1)	0.012(2)
O(8)	0.321(2)	0.431(1)	0.1584(1)	0.010(2)
O(9)	0.177(2)	0.641(1)	0.1108(9)	0.010(2)
O(10)	0.168(2)	0.887(1)	0.468(1)	0.015(2)
O(11)	−0.226(2)	0.556(1)	0.496(1)	0.015(2)
O(12)	0.401(2)	0.960(1)	0.2370(9)	0.009(2)

Table 3
Atomic coordinates and displacement parameters (Å^2) for **2**

Atom	x	y	z	U_{eq}
U(1)	0.0382(1)	0.80059(6)	0.01894(6)	0.0130(2)
U(2)	−0.0194(1)	0.71824(6)	0.47998(6)	0.0135(2)
As(1)	0.2785(3)	0.5817(2)	0.2159(2)	0.0133(4)
As(2)	0.3383(3)	1.1083(2)	0.2716(2)	0.0133(4)
Li(1)	0.747(6)	0.906(3)	0.303(3)	0.014(6)
Li(2)	0.678(7)	0.381(3)	0.231(3)	0.024(7)
O(1)	−0.196(2)	0.816(1)	0.118(1)	0.014(2)
O(2)	0.637(2)	1.259(1)	0.351(1)	0.016(3)
O(3)	0.105(2)	1.110(1)	0.359(1)	0.018(3)
O(4)	0.031(2)	0.558(1)	0.292(1)	0.020(3)
O(5)	0.593(2)	0.709(1)	0.323(1)	0.016(2)
O(6)	0.269(2)	0.783(1)	−0.084(1)	0.015(2)
O(7)	0.177(2)	1.092(1)	0.115(1)	0.021(3)
O(8)	0.325(2)	0.417(1)	0.151(1)	0.017(3)
O(9)	0.173(3)	0.638(1)	0.093(1)	0.026(3)
O(10)	0.185(3)	0.877(1)	0.459(1)	0.030(3)
O(11)	−0.232(3)	0.561(1)	0.497(1)	0.027(3)
O(12)	0.408(2)	0.948(1)	0.236(1)	0.018(3)

Table 1
Crystallographic data and refinement parameters for **1**, **2**, **3** and **4**

Parameters	1	2	3	4
a (Å)	5.0271(1)	5.129(2)	5.051(1)	5.312(1)
b (Å)	9.8799(2)	10.105(3)	5.303(1)	6.696(1)
c (Å)	10.8920(2)	11.080(3)	10.101(1)	12.542(1)
α (deg)	108.282(9)	107.70(2)	90.31(1)	94.532(9)
β (deg)	102.993(8)	102.53(3)	97.49(1)	99.059(8)
γ (deg)	104.13(1)	104.74(3)	105.08(1)	110.189(7)
V (Å^3)	470.69(2)	501.4(3)	258.80(8)	409.17(10)
Space group	$P\bar{1}$	$P\bar{1}$	$P\bar{1}$	$P\bar{1}$
Ref. for cell refinement	All	125	125	All
F_{000}	632	704	352	502
μ (cm^{-1})	347.64	388.68	376.48	301.08
Z	4	4	2	1
D_{calc} (g cm^{-3})	5.249	5.510	5.337	4.756
Crystal size (mm^3)	0.24 × 0.18 × 0.12	0.27 × 0.25 × 0.2	0.35 × 0.32 × 0.2	0.18 × 0.10 × 0.03
Radiation	MoKα	MoKα	MoKα	MoKα
R_{int}	0.0415	0.11	0.0349	0.0296
Total ref.	17982	4989	5444	2359
Unique ref.	3018	2392	2722	1425
Unique ref. $|F_0| \geqslant 4\sigma_F$	2768	1431	2055	1355
R_1	0.0450	0.0550	0.0339	0.0565
wR_2	0.1271	0.1011	0.0726	0.1631
GOOF	1.286	0.990	1.025	1.111
Largest diff. peak/hole	4.362/−2.739	3.993/−2.716	3.907/−1.755	3.555/−3.104

Table 4
Atomic coordinates and displacement parameters ($\mathring{A}^2$) for **3**

Atom	x	y	z	U_{eq}
U(1)	0.5000	0.5000	0.5000	0.04151(4)
U(2)	0.0000	0.0000	1.0000	0.04135(4)
As(1)	0.42481(9)	0.02405(9)	0.74232(4)	0.04172(7)
Li(1)	0.059(2)	−0.550(2)	0.772()	0.060(2)
O(1)	0.2033(6)	−0.1583(6)	0.8365(3)	0.0464(6)
O(2)	0.2313(7)	0.3108(7)	0.9916(4)	0.0516(7)
O(3)	0.4601(8)	−0.1664(7)	0.6190(4)	0.0565(8)
O(4)	0.7364(6)	0.1498(7)	0.8324(3)	0.0478(6)
O(5)	0.1743(6)	0.4840(7)	0.4018(3)	0.0500(6)
O(6)	0.2994(6)	0.2652(6)	0.6755(3)	0.0457(5)

Table 5
Atomic coordinates and displacement parameters ($\mathring{A}^2$) for **4**

Atom	x	y	z	U_{eq}
U(1)	0.0000	0.5000	0.0000	0.0158(1)
U(2)	−0.87805(7)	0.15600(6)	0.37048(3)	0.0146(1)
P(1)	−0.9896(5)	−0.3304(4)	0.3565(2)	0.0138(6)
P(2)	−0.4776(5)	0.4286(5)	0.1864(2)	0.0171(6)
Li(1)	−0.602(4)	−0.074(4)	0.193(2)	0.027(5)
O(1)	−0.987(2)	−0.187(1)	0.4578(6)	0.017(2)
O(2)	−0.307(2)	0.565(1)	0.3013(7)	0.018(2)
O(3)	−0.849(2)	−0.172(1)	0.2858(6)	0.018(2)
O(4)	−0.882(2)	−0.501(1)	0.3759(6)	0.017(2)
O(5)	−1.225(2)	0.054(1)	0.2913(8)	0.024(2)
O(6)	−0.685(2)	0.223(1)	0.2114(7)	0.019(2)
O(7)	−0.616(2)	0.575(1)	0.1334(7)	0.022(2)
O(8)	−0.543(2)	0.2460(2)	0.4444(8)	0.029(2)
O(9)	−0.284(2)	0.383(2)	0.1208(7)	0.026(2)
O(10)	0.046(2)	0.771(2)	0.0406(8)	0.034(2)

Table 6
Selected interatomic distances ($\mathring{A}$) in the structure of **1**

U(1)–O(6)	1.76(1)	P(2)–O(12)	1.53(1)
U(1)–O(1)	1.79(1)	P(2)–O(7)	1.54(1)
U(1)–O(9)	2.23(1)	P(2)–O(2)	1.545(9)
U(1)–O(7)	2.36(1)	P(2)–O(3)	1.55(1)
U(1)–O(8)	2.397(8)		
U(1)–O(12)	2.405(9)	Li(1)–O(12)	1.94(3)
U(1)–O(7)	2.653(9)	Li(1)–O(1)	2.05(3)
		Li(1)–O(5)	2.08(3)
U(2)–O(11)	1.75(1)	Li(1)–O(3)	2.35(3)
U(2)–O(10)	1.77(1)		
U(2)–O(3)	2.27(1)	Li(2)–O(6)	2.01(3)
U(2)–O(5)	2.309(9)	Li(2)–O(8)	2.03(3)
U(2)–O(4)	2.322(9)	Li(2)–O(2)	2.03(3)
U(2)–O(2)	2.436(9)	Li(2)–O(4)	2.05(3)
P(1)–O(9)	1.51(1)		
P(1)–O(8)	1.54(1)		
P(1)–O(5)	1.549(9)		
P(1)–O(4)	1.55(1)		

Table 7
Selected interatomic distances ($\mathring{A}$) in the structure of **2**

U(1)–O(1)	1.79(1)	As(2)–O(2)	1.69(1)
U(1)–O(6)	1.82(1)	As(2)–O(7)	1.69(1)
U(1)–O(9)	2.24(1)	As(2)–O(12)	1.70(1)
U(1)–O(7)	2.34(1)	As(2)–O(3)	1.70(1)
U(1)–O(8)	2.40(1)		
U(1)–O(12)	2.45(1)	Li(1)–O(12)	1.96(3)
U(1)–O(7)	2.65(1)	Li(1)–O(1)	2.04(3)
		Li(1)–O(5)	2.13(3)
U(2)–O(11)	1.77(1)	Li(1)–O(3)	2.18(3)
U(2)–O(10)	1.79(1)		
U(2)–O(3)	2.27(1)	Li(2)–O(8)	1.97(3)
U(2)–O(4)	2.30(1)	Li(2)–O(4)	2.04(3)
U(2)–O(5)	2.30(1)	Li(2)–O(6)	2.06(3)
U(2)–O(2)	2.30(1)	Li(2)–O(2)	2.13(3)
As(1)–O(9)	1.67(1)		
As(1)–O(5)	1.69(1)		
As(1)–O(8)	1.70(1)		
As(1)–O(4)	1.70(1)		

Table 8
Selected interatomic distances ($\mathring{A}$) in the structure of **3**

U(1)–O(5)	1.789(3)	As(1)–O(3)	1.656(4)
U(1)–O(5)	1.789(3)	As(1)–O(6)	1.677(3)
U(1)–O(3)	2.200(4)	As(1)–O(1)	1.679(3)
U(1)–O(3)	2.200(4)	As(1)–O(4)	1.681(3)
U(1)–O(6)	2.357(3)		
U(1)–O(6)	2.357(3)	Li(1)–O(5)	2.06(1)
		Li(1)–O(6)	2.07(1)
U(2)–O(2)	1.765(4)	Li(1)–O(1)	2.09(1)
U(2)–O(2)	1.765(4)	Li(1)–O(4)	2.12(1)
U(2)–O(4)	2.290(3)		
U(2)–O(4)	2.290(3)		
U(2)–O(1)	2.315(3)		
U(2)–O(1)	2.315(3)		

Table 9
Selected interatomic distances ($\mathring{A}$) in the structure of **4**

U(1)–O(10)	1.77(1)	P(1)–O(4)	1.467(8)
U(1)–O(10)	1.77(1)	P(1)–O(3)	1.511(8)
U(1)–O(9)	2.298(8)	P(1)–O(1)	1.528(8)
U(1)–O(9)	2.298(8)	P(1)–O(2)	1.599(8)
U(1)–O(7)	2.303(8)		
U(1)–O(7)	2.303(8)	P(2)–O(9)	1.506(9)
		P(2)–O(7)	1.531(8)
U(2)–O(8)	1.745(9)	P(2)–O(6)	1.543(8)
U(2)–O(5)	1.814(8)	P(2)–O(2)	1.593(8)
U(2)–O(4)	2.297(8)		
U(2)–O(6)	2.387(8)	Li(1)–O(3)	1.86(2)
U(2)–O(1)	2.389(8)	Li(1)–O(5)	2.01(2)
U(2)–O(3)	2.428(8)	Li(1)–O(6)	2.22(2)
U(2)–O(1)	2.546(8)	Li(1)–O(7)	2.32(2)
		Li(1)–O(10)	2.36(2)

bipyramidal. The U^{6+} cations form linear uranyl groups UO_2^{2+}, with the U–O bond lengths in the range of 1.75–1.82 Å. The equatorial U^{6+}–O bond lengths in the UO_6 and UO_7 bipyramids ranges from 2.27 to 2.44 and 2.23–2.66 Å, respectively. In the structure of **3**, U atoms form square bipyramids only. The U^{6+}–O distances range from 1.765 to 1.789 Å for uranyl groups and from 2.200 to 2.357 Å for equatorial ligands.

The P and As atoms have tetrahedral coordination. In **1**, **2**, and **3**, TO_4 tetrahedra are isolated from each other, whereas, in **4**, PO_4 tetrahedra form dimeric P_2O_7 groups. Bond lengths and angles in the PO_4 tetrahedra are in the range from 1.47 to 1.59 Å and 103–116.1°, respectively. For the AsO_4 tetrahedra, the observed As–O bond lengths vary from 1.65 to 1.70 Å, whereas the angles vary from 99.8° to 112.2°.

The Li atoms in the structures of **1**, **2**, and **3**, have four-fold coordination with the Li^+–O distances 1.94–2.35 Å. In the structure of **4**, Li atoms have fivefold coordination (Li–O = 1.86–2.36 Å).
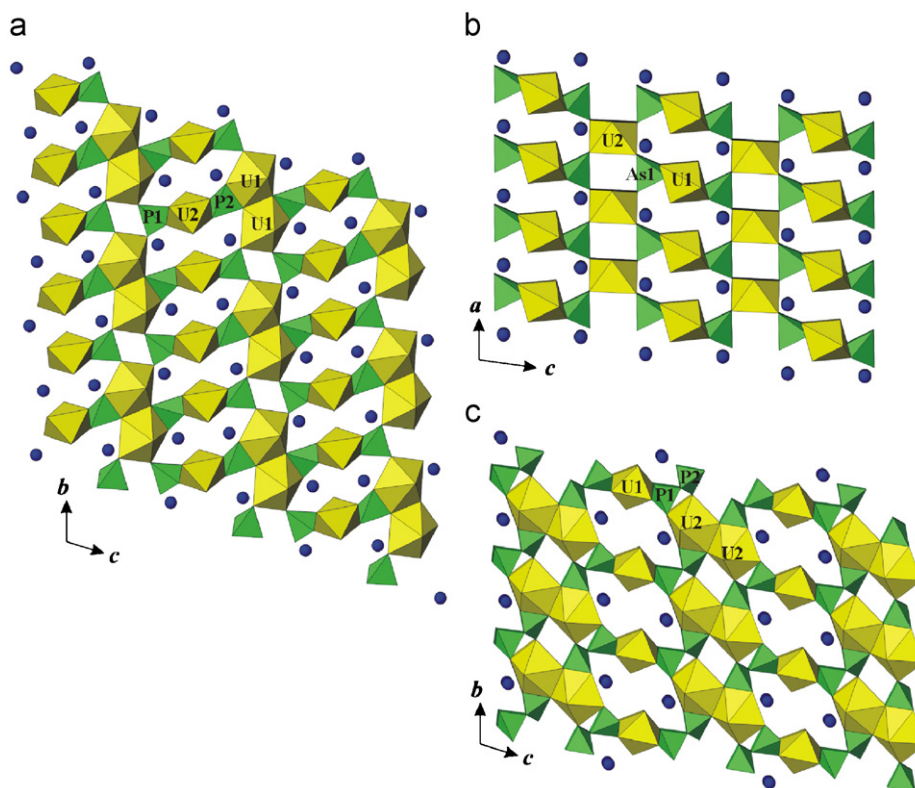
Fig. 1. Crystal structures of the title compounds: structures of **1** and **2** (a), **3** (b), and **4** (c). Legend: U polyhedra = yellow, TO_4 tetrahedra (T = P, As) = green, Li$^+$ cations = blue circles.

3.2. Bond-valence analysis

Bond-valence sums have been calculated using bond-valence parameters provided by Burns et al. [15] for the U^{6+}–O bonds and by Brese and O'Keeffe [16] for other bonds. The bond-valence sums for the U sites are in the wide range of 5.56–6.03 v.u. (valence units), The bond-valence sums for P (in **1** and **4**) and for As (in **2** and **3**) sites are from 4.74 to 4.97 v.u. and from 4.86 to 5.16 v.u., respectively. The bond-valence sums for the Li sites and the O sites are in the ranges of 0.75–0.89 and 1.65–2.10 v.u., respectively.

3.3. Structure description

Fig. 1 shows structure diagrams for the title compounds. Their structures are based upon 3-D frameworks of U and P polyhedra. The compounds **1** and **2** are isostructural. The heteropolyhedral framework (Fig. 1a) is based upon U_2O_{12} dimers of edge-sharing UO_7 bipyramids, UO_6 square bipyramids and isolated $P(As)O_4$ tetrahedra. The structure of **3** consists of framework of corner-sharing UO_6 and arsenate tetrahedra (Fig. 1b). The framework of **4** is more complex than those in the other materials. It is based upon the U_2O_{12} dimers, UO_6 square bipyramids and P_2O_7 tetrahedral dimers (Fig. 1c). In all the compounds studied, Li$^+$ cations reside in framework cavities and compensate negative charge of the anionic frameworks.

4. Discussion

The phases **1**, **2** and **3** have the same U/T ratio (T = P, As) as a large group of natural and synthetic uranyl phosphates or arsenates [1,3]. However, most of the phases of this group are hydrated that has a dramatic influence upon the structural architecture. In fact, hydrated chemical analogues of **1**, **2** and **3** are $Li[(UO_2)(PO_4)](H_2O)_4$ and $Li[(UO_2)(AsO_4)](H_2O)_4$, which crystallize in the meta-autunite structure type [5,17]. Among natural phases, dimers U_2O_{12} of edge-sharing uranyl bipyramids present in **1**, **2** and **4** have been observed in the 1-D chain structures of parsonsite and hallimondite $Pb[(UO_2)(TO_4)](H_2O)_n$ [18,19], but have not been seen in any uranyl-based 2D and 3D structures. The phase **4** has a ratio of U/T = 3:4 that is unique in uranyl phosphate and arsenate chemistry. Recently, Obbade et al. [20] reported synthesis and structure of $Li_2[(UO_2)_3(VO_4)_2O]$ that has the U/T ratio of 4:3, i.e. U/T > 1. As a consequence of the difference in chemical composition, structure of this phase is drastically different from the structures of compounds reported herein.

The structure topology of the heteropolyhedral frameworks of the compounds studied can be investigated using nodal representation. Within this approach developed in details in [21–23], U and P polyhedra are symbolized by black and white nodes, respectively. The nodes are linked by a single edge when respective polyhedra share a common apex (one anion) and by a double edge if they share an edge (two anions). Fig. 2 shows 3D graphs that correspond to the topologies of polyhedral linkages in **3** (Fig. 2a) and **1** and **2** (Fig. 2b). The graph shown in Fig. 2a can be easily recognized as the framework corresponding to the atomic arrangement in PtS (cooperite). The cooperite network is a common topology for a wide range of inorganic and metal-organic compounds [24–27]. It can be described as built by cross-linkage of chains of edge-sharing squares centered by black vertices. As a result, each black vertex has square coordination, whereas each white vertex has distorted tetrahedral coordination. The chains of black-centered squares
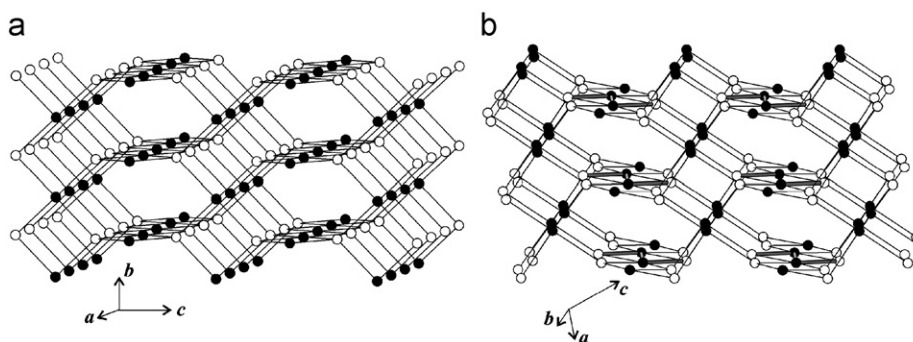
Fig. 2. Black-and-white graphs describing topology of heteropolyhedral frameworks in **3** (a) and in **1** and **2** (b). See text for details.
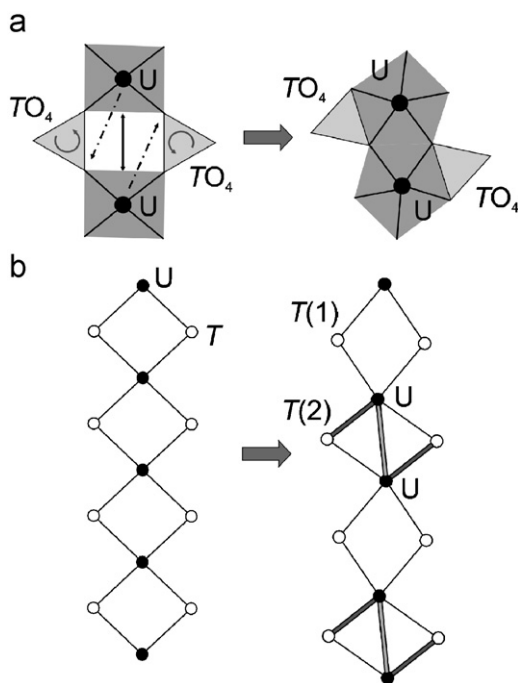

Fig. 3. Transition between the frameworks shown in Fig. 2a and b described in terms of coordination polyhedra (a) and 1-D graphs (b). See text for details.

can be provisionally subdivided into vertical and horizontal ones.

The graph of **3** consists of single edges only that corresponds to the linkage of UO_6 and AsO_4 polyhedra via common corners only. The graph of the framework present in **1** and **2** (Fig. 2b) contains double edges between some black and between some black and white vertices. This feature describes the formation of dimers of UO_7 bipyramids and edge-sharing between UO_7 bipyramids and PO_4 tetrahedra. However, the overall architecture follows the arrangement of nodes in the cooperite network. The transition from the latter to the graph shown in Fig. 2b involves reconstruction of horizontal chains of squares by addition of double edges between black vertices and replacement of some single edges between black and white vertices by double edges. It is important that, during this process, vertical chains of squares do not experience any topological reconstruction. Fig. 3 provides a description of this transition in terms of coordination polyhedra (Fig. 3a) and in terms of graphs (Fig. 3b). In the phase **3**, adjacent UO_6 bipyramids are linked via two TO_4 tetrahedra (Fig. 3a). The

transformation process involves formation of additional U–O bond by each U atom in the pair. As a result, a UO_6 square bipyramid is transformed into a UO_7 pentagonal bipyramids, and edge-sharing between U and U, and U and P polyhedra appear (Fig. 3a). Fig. 3b describes the same transformation in terms of 1D graphs of black and white vertices that represent portions of the networks shown in Fig. 2. In the structure of **3**, black and white vertices are linked by single edges only and no black–black linkage are observed (Fig. 3b). Formation of additional U–O bonds and edge linkage between polyhedra results in appearance of **Z**-shaped arrangements of double edges (Fig. 3b).

Fig. 4a shows a black-and-white graph that symbolizes the topology of heteropolyhedral framework in the structure of **4**. Again, it can be described as consisting of vertical and horizontal chains. The vertical chains are of the cooperite type and formed by squares centered by black vertices. In contrast, horizontal chains have a different topology (Fig. 4b). They are formed by edge sharing of squares formed by two white and two black vertices. It is interesting that **Z**-shaped fragments of double edges are present here as well. However, there is no simple topological transition from the cooperite net to the net shown in Fig. 4a. This is undoubtedly a consequence of the fact that the ratio of black and white vertices in the net is 3:4 and not 1:1 as in the cooperite net. Thus, topological reconstruction should include the insertion of an additional white vertex in topological space corresponds to the replacement of PO_4 tetrahedra by P_2O_7 dimers in real space. In general, there are obvious topological similarities between the graph in Fig. 4a and the cooperite net but transition from one graph to the other involves fundamental recombination and insertion of additional elements.

5. Conclusion

The results presented here demonstrate that anhydrous uranyl phosphates and arsenates display a wide range of topological variations that manifest itself in the formation of polymorphs with different (though closely related) structures. The phases reported here are based upon 3D frameworks with topologies that can be derived from the cooperite net by a series of topological operations such as insertion of new edges or vertices and modification of the system of edges. The same series of transformations can also be seen for a number of 2D structures observed in inorganic oxysalts [23]. It is worthy to note that the compounds **2** and **3** reported here represent another example of combinatorial polymorphism in uranyl phosphates and arsenates. The first observation of this kind have been recently reported for α, β-K[(UO$_2$)(PO$_3$)$_3$], two compounds containing polyphosphate tetrahedral chains [14].
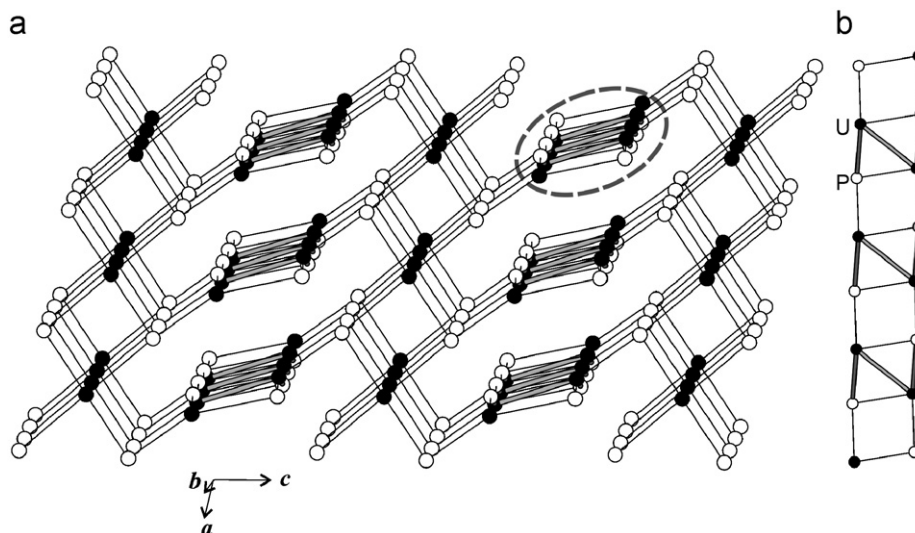
Fig. 4. Black-and-white graph describing topology of heteropolyhedral framework in **4** (a) and topology of horizontal chain (b).

Acknowledgment

Appendix A. Supporting Information

Supplementary data associated with this article can be found in the online version at doi:10.1016/j.jssc.2008.07.028.

References

[1] S.V. Krivovichev, P.C. Burns, I.G. Tananaev (Eds.), Structural Chemistry of Inorganic Actinide Compounds, Elsevier, Amsterdam, 2007.
[2] P.C. Burns, Can. Mineral. 43 (2005) 1839.
[3] R. Finch, T. Murakami, Rev. Mineral. 38 (1999) 91.
[4] P.C. Burns, M.L. Miller, R.C. Ewing, Can. Mineral. 34 (1996) 1551.
[5] A. Locock, in: S.V. Krivovichev, P.C. Burns, I.G. Tananaev (Eds.), Structural Chemistry of Inorganic Actinide Compounds, Elsevier, Amsterdam, 2007, p. 217.
[6] S.A. Linde, Yu.E. Gorbunova, A.V. Lavrov, V.G. Kuznetsov, Dokl. Akad. Nauk. SSSR 242 (1978) 1083.
[7] S.A. Linde, Yu.E. Gorbunova, A.V. Lavrov, Zh. Neorg. Khim. 25 (1980) 1992.
[8] S.A. Linde, Yu.E. Gorbunova, A.V. Lavrov, A.B. Pobedina, Izv. Akad. Nauk. SSSR Neorg. Mater. 17 (1981) 1062.
[9] S.A. Linde, Yu.E. Gorbunova, A.V. Lavrov, A.B. Pobedina, Zh. Neorg. Khim. 29 (1984) 1533.
[10] Yu.E. Gorbunova, S.A. Linde, A.V. Lavrov, A.B. Pobedina, Dokl. Akad. Nauk. SSSR 251 (1980) 385.
[11] A.B. Pobedina, A.B. Ilyukhin, Zh. Neorg. Khim. 42 (1997) 1120.
[12] E.V. Alekseev, S.V. Krivovichev, W. Depmeier, Acta Crystallogr. A 63 (2007) s30.
[13] E.V. Alekseev, S.V. Krivovichev, W. Depmeier, Z. Anorg. Allg. Chem. 633 (2007) 1125.
[14] E.V. Alekseev, S.V. Krivovichev, W. Depmeier, Z. Anorg. Allg. Chem. 634 (2008) 1527.
[15] P.C. Burns, R.C. Ewing, F.C. Hawthorne, Can. Mineral. 35 (1997) 1551.
[16] N.E. Brese, M. O'Keeffe, Acta Crystallogr. B 47 (1991) 192.
[17] A.J. Locock, P.C. Burns, M.JM. Duke, T.M. Flynn, Can. Mineral. 42 (2004) 973.
[18] P.C. Burns, Am. Mineral. 85 (2000) 801.
[19] A.J. Locock, P.C. Burns, T.M. Flynn, Am. Mineral. 90 (2005) 240.
[20] S. Obbade, L. Duvieubourg, C. Dion, F. Abraham, J. Solid State Chem. 180 (2007) 866.
[21] S.V. Krivovichev, Crystallogr. Rev. 10 (2004) 185.
[22] S.V. Krivovichev, Rev. Mineral. Geochem. 57 (2005) 17.
[23] S.V. Krivovichev, Structural Crystallography of Inorganic Oxysalts, Oxford University Press, Oxford, 2008 in press.
[24] L. Carlucci, G. Ciani, D.W. Gudenberg, D.M. Proserpio, New J. Chem. 33 (1999) 397.
[25] M. O'Keeffe, M. Eddaoudi, H. Li, T. Reineke, O.M. Yaghi, J. Solid State Chem. 152 (2000) 3.
[26] O. Delgado-Friedrichs, M. O'Keeffe, O.M. Yaghi, Solid State Sci. 5 (2003) 73.
[27] B. Chen, N.W. Ockwig, F.R. Fronczek, D.S. Contreras, O.M. Yaghi, Inorg. Chem. 44 (2005) 181.